JBUON 2016; 21(1): 125-134
ISSN: 1107-0625, online ISSN: 2241-6293 • www.jbuon.com
E-mail: editorial_office@jbuon.com

ORIGINAL ARTICLE

In vitro and *in vivo* effect of paclitaxel and cepharanthine co-loaded polymeric nanoparticles in gastric cancer

Hai-Hua Yu[1*], Wen-Ning Mi[2*], Bo Liu[1], Hong-Peng Zhao[1]

[1]Department of Gastrointestinal Surgery, Shandong Provincial Qian Foshan Hospital, Jinan, Shandong 250014, China;
[2]Department of Surgery, No.456 Hospital of the PLA Jinan Military Region, Jinan, Shandong 250031, China

*These authors contributed equally to this work

Summary

Purpose: *Response surface methodology (RSM) using the central composite rotatable design (CCRD) model was used to optimize the formulation of paclitaxel (PTX)-cepharanthine (CEP) nanoparticles for gastric cancer.*

Methods: *Nanoparticles were prepared using nanoprecipitation technique and optimized using central composite rotatable design response surface methodology (CCRD-RSM). Further the optimized nanoparticles were characterised for particle size (PS), zeta potential, entrapment efficiency (EE), drug loading efficiency (DL), anticancer potential against MKN45 (human gastric cancer) cells, in vivo tumor inhibition and survival analysis.*

Results: *Significant findings were the optimal formulation of polymer concentration of 48 mg, surfactant concentration of 45% and EE of 98.12%, DL of 15.61% and mean diameter of 198±4.7 nm. The encapsulation of PTX/CEP into nanoparticles retained the synergistic anticancer efficiency against MKN45 cells. In the in vivo evaluation, PTX/CEP nanoparticles delivered into mice by intravenous injection significantly improved the antitumor efficacy of PTX/CEP. Moreover, PTX/CEP co-loaded nanoparticles substantially increased the overall survival in an established MKN45-transplanted mouse model.*

Conclusion: *These data are the first to demonstrate that PTX/CEP co-loaded nanoparticles increased the anticancer efficacy in cell lines and xenograft mouse model. Our results suggest that PTX/CEP coloaded nanoparticles could be a potential useful chemotherapeutic formulation for gastric cancer.*

Key words: *cepharanthine, gastric cancer, nanoparticle, paclitaxel, response surface methodology*

Introduction

Gastric cancer is the fourth leading cause of cancer-related deaths worldwide, and peritoneal dissemination is the most frequent and life-threatening form of metastasis and recurrence in patients with gastric cancer [1,2]. The current systemic chemotherapy regimens for gastric cancer are rather unsatisfactory. Current research into drug delivery systems (DDS) is mostly aimed at improving the penetration of drugs into tumors or prolonging the retention of drugs in the peritoneal cavity [3,4].

PTX is one of the most widely used anticancer agents and has demonstrated extraordinary activities against a variety of solid tumors. PTX exerts its cytotoxicity by disrupting cell functions through accelerating the microtubule assembly from tubulin and blocking the depolymerization of the microtubule, which eventually causes a G_2-M cell arrest [5]. Recent clinical trials have demonstrated the advantage of PTX in combination with other anticancer agents in the treatment of hepatocellular carcinoma [6,7]. However, the therapeutic response of PTX is often associated with severe side effects caused by its nonspecific cytotoxic effects and special solvents (Cremophor EL®) [8,9]. Therefore, there is a need to focus

Correspondence to: Hong-Peng Zhao, MD. Department of Gastrointestinal Surgery, Shandong Provincial Qian Foshan Hospital, No.16766 Jingshi Road, Jinan, Shandong 250014, China. Tel & Fax: +86 531 82968900, E-mail: hpzhao54@gmail.com
Received: 16/06/2015; Accepted: 20/07/2015

in the field of cancer therapy to search for novel strategies in order to achieve higher antitumor efficacy of PTX.

CEP is a biscoclaurine alkaloid isolated from Stephania cepharantha, and is used in traditional Chinese medicine as an antirheumatic, antiinflammatory, and antihypertensive agent [10]. Recent studies have shown that CEP exhibited antitumor effects *in vitro* and *in vivo* [11]. Moreover, a recent study has reported multidrug resistance reversal of CEP in cancer cells and animal models [12]. CEP could synergistically increase the cytotoxicity of PTX against gastric cancer cells. These findings suggested the potential of CEP to be a novel adjunct to chemotherapy.

Failure of clinical cancer therapy is attributed mainly to the following two aspects. The technical difficulty for successful chemotherapy is the site-specific delivery of adequate chemotherapeutics to the tumor site with minimal undesirable systemic toxicities. Recently, biodegradable polymeric nanoparticles composed of amphiphilic copolymers have attracted intense interest as a promising tumor-targeted drug delivery system [13,14]. The characteristic structure of amphiphilic copolymers enable themselves to self-assemble into nanoscaled core-shell spherical structures with the hydrophobic part (eg, poly(-caprolactone) [PCL]) as the inner core and the hydrophilic part (eg, poly(ethylene glycol) [PEG]) as the outer shell. Therefore, the hydrophobic core is easy to incorporate the lipophilic drugs, which exhibits a sustained manner of drug release by slow degradation of the polymer. The outer shell formed by the hydrophilic part (PEG) enables the nanoparticles to escape from the scavenging of the reticuloendothelial systems effectively, thereby leading to a long circulation time *in vivo* [15].

Moreover, nanoparticulate drug delivery systems were proven to be preferentially located in the tumor tissue by enhanced permeability and retention effect [16]. However, systemic administration failed to achieve high drug concentration in the tumor, although it seems that the antitumor effect was augmented, in addition to reduced side effects [17]. Accordingly, local-regional chemotherapy has emerged as an effective method to eradicate tumors. The drug-loaded nanoparticles are characterized by controlled release of the incorporated drugs as compared to free drugs, which may overcome the deficiency of drug retention in the tumor and may reach a satisfying outcome in improving antitumor efficacy when combined with intratumoral delivery. Previous work in the authors' laboratory has demonstrated the enhanced anticancer effect of cisplatin-loaded nanoparticles against liver cancer by intratumoral delivery [13]. Furthermore, since chemoresistance to PTX correlates with intracellular antioxidant capacity, co-delivery of PTX and CEP generate a synergistic antitumor effect. Based on the findings above, it has been demonstrated that the co-administration of PTX and CEP by nanoparticles leads to more intracellular reactive oxygen species induction, which could efficiently enhance the cytotoxicity of PTX by sequential inhibition of the reactive oxygen species-dependent Akt pathway and activation of apoptotic pathways [18].

The purpose of the current study was to provide a novel therapeutic strategy that could amplify the antitumor effect of PTX by employing CEP, a traditional Chinese medicine as a modulator. This novel approach utilizes polymeric nanoparticles as drug carriers for the codelivery of PTX and CEP intravenously for optimal therapeutic efficacy. Biodegradable core-shell methoxy PEG-PCL nanoparticles incorporating PTX and CEP simultaneously were prepared, and the *in vivo* efficacy was examined through intravenous administration.

Methods

Materials

PTX, CEP, 3-(4, 5-dimethylthiazol-2-yl)-2, 5-diphenyltetrazolium bromide (MTT) were purchased from Sigma-Aldrich Corporation, Shanghai, China. All other chemicals were of analytical grade and used without further purification. Human gastric cancer cell line MKN45 was obtained from Shanghai Institute of Cell Biology (Shanghai, China). The cells were cultured in RPMI-1640 medium with 10% foetal bovine serum and 100 U/mL penicillin-streptomycin at 37°C in a water-saturated atmosphere with 5% CO_2.

Formulation of nanoparticles

PTX/CEP-coloaded nanoparticles were prepared by a nanoprecipitation method [18]. Briefly, a pre-determined amount of methoxy PEG-PCL block copolymers, CEP and PTX were dissolved in an aliquot of acetone. The obtained organic solution was added dropwise into 10 different volumes of distilled water under gentle stirring at room temperature. The solution was dialyzed in a Spectra POR2 dialysis membrane (Spectrum Lab, Houston, TX) (molecular weight cut off 12 kDa) to thoroughly remove the acetone. The resulted bluish aqueous solution was filtered through a 0.22-μM filter membrane (GVWP04700; Millipore, Billerica, MA) to remove non-incorporated drugs and copolymer aggregates. Drug-free nanoparticles were produced in a sim-

Table 1. Independent variables and their corresponding levels of nanoparticle preparation for CCRD

	Levels				
Variables	*-1.682*	*-1*	*0*	*+1*	*+1.682*
Polymer concentration	-3.63586	10	30	50	63.6359
Surfactant concentration	-0.0056723	0.25	0.62	1	1.25567
Stirring time	19.7731	30	45	60	70.2269

ilar way by eliminating drugs. Solutions of drug-loaded nanoparticles and empty nanoparticles were then lyophilized for further utilization. The feeding ratio of nanoparticles to cryoprotectant was 1:5, with Pluronic® F68 (BASF, Ludwigshafen, Germany) as the cryoprotectant.

Experimental design

Preliminary experiments indicated that the variables, including polymer concentration, surfactant concentration and stirring time were the main factors that affected the PS, size distribution, DL percentage and encapsulation efficiency of the PTX/CEP nanoparticles. Thus, CCRD-RSM was used to systemically investigate the influence of these three critical formulation variables on particle size, DL percentage (%,w/w) and EE (%,w/w) of the prepared nanoparticles. The details of the design are listed in Table 1. For each factor, the experimental range was selected on the basis of the results of preliminary experiments and the feasibility of preparing the nanoparticles at the extreme values. The value range of the variables was polymer concentration (X1) of 10-50 mg, surfactant concentration (X2) of 0.25-1%, and stirring time (X3) of 30-60 min. A total of 20 tests were conducted. All the formulations in these experiments were prepared in duplicate.

Characterization of nanoparticles

Particle size and Zeta potential

The mean diameter and size distribution were measured before lyophilization by photon correlation spectroscopy (dynamic light scattering) (BI-9000AT; Brookhaven Instruments Corporation, Holtsville, NY). Zeta potential was measured by laser Doppler anemometry (ZetaPlus; Brookhaven Instruments).

Drug loading (DL) capacity and entrapment efficiency (EE)

The concentration of PTX and CEP were assayed on an LC-10 AD high-performance liquid chromatography system (Shimadzu Corporation, Tokyo, Japan) equipped with a Shimadzu ultraviolet detector and an Agilent C-18, 5 μM, 200 mm×4.6 mm reversed-phase high- performance liquid chromatography analytical column (Agilent Technologies, Santa Clara, CA). The mobile phase for CEP consisted of methanol (spectral grade; Merck KGaA, Darmstadt, Germany)/double-distilled water/ethylamine (90/10/0.05 volume/volume/volume) pumped at a flow rate of 1.0 mL/min with a determination wavelength of 282 nm. The concentration of CEP was determined based on the peak area at the retention time of 4.83 min by reference to a calibration curve. The mobile phase for detecting PTX consisted of acetonitrile (spectral grade; Merck)/double-distilled water (58/42 volume/volume) pumped at a flow rate of 1.0 mL/min with a determination wavelength of 228 nm. The concentration of PTX was determined based on the peak area at the retention time of 7.3 min by reference to a calibration curve.

The following equations were applied to calculate the DL and EE:

DL (%) = Weight of the drug in nanoparticles/ weight of the nanoparticles × 100

EE (%) = Weight of the drug in nanoparticles/ weight of the feeding drugs × 100

In vitro cytotoxicity studies

The *in vitro* drug-induced cytotoxic effects were measured by MTT reduction assay. MKN45 cells were seeded at a density of $1x10^4$ cells/well and immediately exposed to a series of doses of free PTX alone and of combination of PTX/CEP nanoparticles with dimethyl sulfoxide (DMSO) treatment (concentration , 0.1%) as a negative control at 37°C. After treatment, 0.1% volume of MTT was added to each well and the plate was further incubated at 37°C for another 4 hrs. DMSO (200 μL) was added to each well to solubilize the MTT-formazan product after removal of the medium. Absorbance at 570 nm was measured with a multiwell spectrophotometer (BioTek, Winooski, VT). Growth inhibition was calculated as a percentage of the untreated controls, which were not exposed to drugs.

Evaluation of antitumor effect and survival analysis

Male Wistar albino mice of 6-8 weeks of age and weighing 18-22 g were obtained from the animal house of Shandong Provincial Qian Foshan Hospital, Jinan, Shandong, China and raised in a specific pathogen-free facility for *in vivo* experiments with the following guidelines: all animal procedures were approved, controlled by the local ethics committee and carried out according to the guidelines of Chinese law concerning protection of animal life. The mice were housed at 22°C with a relative humidity of 40-60% and a 12-hr light/12-hr dark cycle. The MKN45 cells at density of

Table 2. Central composite design consisting of experiments for the study of three experimental factors in coded levels with experimental results

Formulation	Coded value variables			Response values		
	X_1	X_2	X_3	EE (%)	DL (%)	PS (nm)
1	10.00	0.25	30.00	70	13	237
2	50.00	0.25	30.00	96	4	242
3	10.00	1.00	30.00	90	13	238
4	50.00	1.00	30.00	71	4	249
5	10.00	0.25	60.00	72	12	110
6	50.00	0.25	60.00	90	5	106
7	10.00	1.00	60.00	90	12	108
8	50.00	1.00	60.00	91	5	102
9	-3.64	0.63	45.00	91	14	146
10	63.64	0.63	45.00	96	5	151
11	30.00	-0.01	45.00	62	4	148
12	30.00	1.26	45.00	68	3	147
13	30.00	0.63	19.77	62	5	263
14	30.00	0.63	70.23	94	4	110
15	30.00	0.63	45.00	90	3	147
16	30.00	0.63	45.00	90	3	147
17	30.00	0.63	45.00	90	3	147
18	30.00	0.63	45.00	90	3	147
19	30.00	0.63	45.00	90	3	147
20	30.00	0.63	45.00	90	3	147

EE: entrapment efficiency, DL: drug loading, PS: particle size

$1x10^6$ were injected into each mouse subcutaneously at the mammary fat pad near the left armpit. The xenografts were visible 7 days after injection of the cells. Tumor volume (V) was calculated by the formula: V = 1/2 (length × width^2).

Eleven days post-injection of the cells, 57 mice (weighing 20.7±1.9 g) with locally isolated tumors (diameter 5.5–6.5 mm) were selected and randomly divided into three groups for evaluation of tumor inhibition. The mice were injected via the tail vein with 0.4 mL of saline (control) or 0.4 mL of saline solutions containing PTX and PTX/CEP nanoparticle, respectively, with an equivalent PTX dose of 20 mg/kg. Then, on day 13 post-injection of cells, 75 mice (weighing 20.8±1.7g) with locally isolated tumors (diameter of 6.5–7.4mm) from the rest models were randomly divided into three groups and treated similarly, as above. The mouse survival rate in each group was recorded daily and censored at day 75 after drug administration.

Hematoxylin and eosin staining of tumor slices

For histology observation, formalin-fixed tumor tisues were cut into 4-μm thick slices and stained with hematoxylin and eosin (Sigma-Aldrich Inc). Finally, the slides were examined by optical microscopy.

Statistics

The data are presented as the mean ± standard deviation and were analyzed using SPSS version 16.0 (SPSS Inc, Chicago, ILL). Comparison of data between the different groups was tested by one-way analysis of variance (ANOVA). Kaplan-Meier survival plots were generated and comparisons between the survival curves were made using the log-rank test. A p value<0.05 was considered to be statistically significant.

Results

Optimization

The variables shown in Table 1 were chosen based on our preliminary experiments.

Table 2 shows the experimental results concerning the tested variables on drug EE, DL percentage and mean diameter of PS. The three dependent values ranged from 56 to 96% by weight, 3 to 14% by weight and 102 to 263 nm, respectively. A mathematical relationship between factors and parameters was generated by response surface regression analysis using Design-Expert® 7.0 software. The three-dimensional (3D)

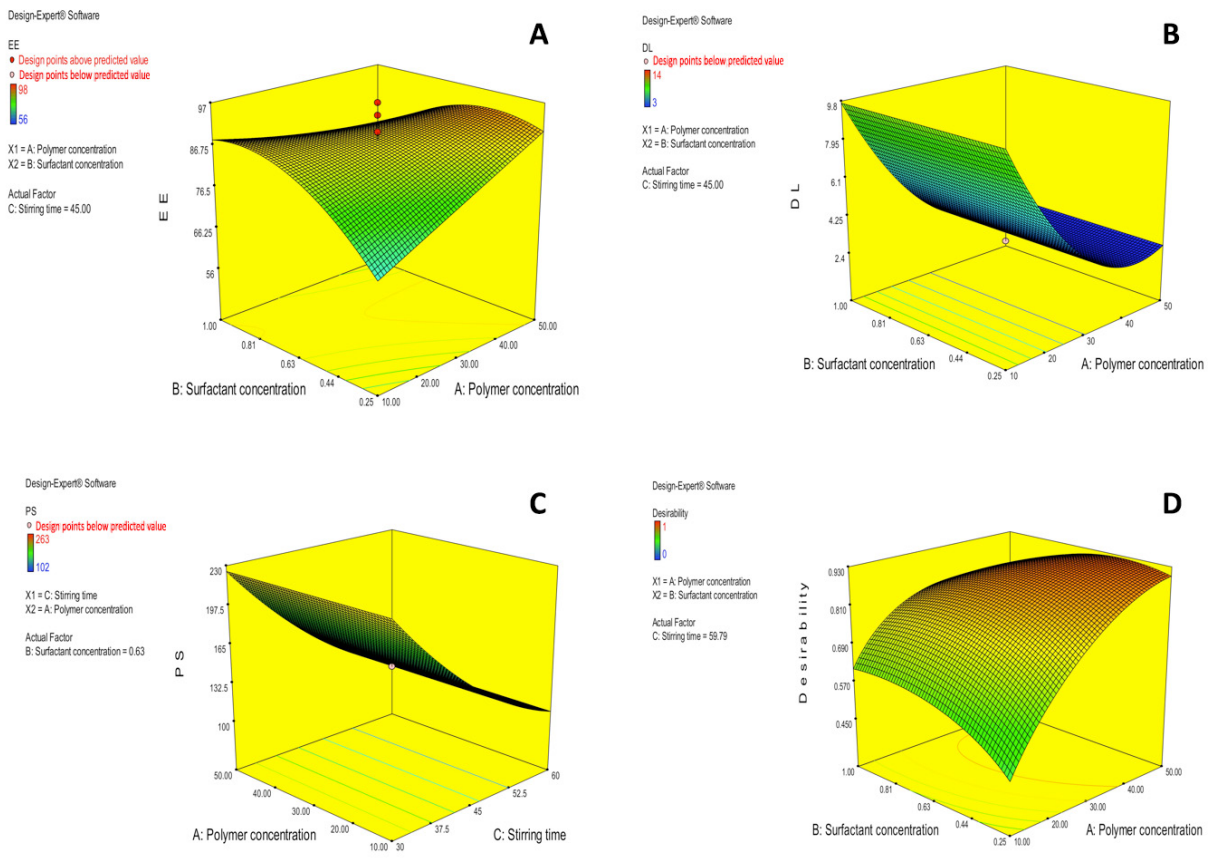

Figure 1. Three dimensional (3D) response surface plots showing the effect of the variable on response. (**A**): The effect of polymer and surfactant concentration on the entrapment efficiency; (**B**): The effect of polymer and surfactant concentration on the drug loading; (**C**): The effect of polymer concentration and stirring time on particle size; (**D**): Overall desirability graph D value=0.930.

Table 3. Comparison of experimental and predicted values under optimal conditions for final formulation

Polymer concentration (mg)	*Surfactant concentration (%)*	*Stirring time (min)*	*Particle size (nm)*	*Entrapment efficiency (%)*	*Drug loading (%)*
48	0.48	60			
Predicted			196.5	97.8	15.0
Experimental			198.2	98.4	15.3
Bias (%)			0.8	0.6	1
Acceptance criteria = 2%					

Bias was calculated as (predicted value-experimental value)/predicted value ×100

response surface graphs for the most statistically significant variables on the evaluated parameters are shown in Figure 1. The response surface diagrams show the higher polymer and surfactant concentrations (higher in EE and lower in DL). Furthermore, the PS significantly decreased the stirring time. The optimized variables showed a good fit to the second-order polynomial equation with correlation coefficient (r) of 0.9359, 0.9944 and 0.9309, respectively. After model simplification with backward stepwise solution, the r value decreased slightly to 0.8837, 0.9923, and 0.9212, respectively. The lack-of-fit was not significant at 95% confidence level. All the remaining parameters were significant at $p<0.05$. The statistical analysis of the results generated the following polynomial equations:

$$EE=+88.44+2.52xA+1.76xB-7.75xAB-7.09xB2$$

$$DL=+3.50-3.45xA-0.12xC+2.75xA2+0.99xC2$$

$$PS=+151-58.38xC+16.03xC2$$

where X1, X2 and X3 (standing for A, B and C, re-

Table 4. Mean ± standard deviation for volume and net weight of MKN45 xenograft tumors on day 12 after initial treatment

Group	*N*	*Volume (mm^3)*	*TIR (%)*	*Net weight (g)*	*TIR (%)*
Control	14	562 ±264▲		0.52 ±0.18▲	
PTX	14	321±175*,▲	39.8	0.41±0.21*,	22.2▲
PTX/CEP nanoparticles	15	154±132*	73.2	0.24±0.12*	62.8

Volume data: *p < 0.01 vs control; ▲p<0.01 vs PTX/CEP nanoparticles; p=0.812 PTX vs PTX/CEP nanoparticles; Weight data: *p<0.01 vs control; ▲p<0.01 vs PTX/CEP nanoparticles; p=0.017, control vs PTX; p=0.097. PTX vs PTX/CEP nanoparticles

Table 5. Mean survival time

Group	*N*	*Mean ±SD (days)*	*95%CI (days)*	*Mean ±SD (days)*	*95%CI (days)*
Control▲▲	25	41.0±2.2	36.2-44.4	41.7±2.2	35.4-45.9
PTX*▲▲	25	45.0±1.2	41.6-46.5	47.3±1.8	43.4-54.2
PTX/CEP nanoparticle**▲	25	58.0±4.6	46.2-64.2	58.4±1.2	48.0-56.5

Log-rank test (Mantel-Cox): *p=0.03; ** p<0.001 vs control; ▲p=0.025, ▲▲p<0.001, compared with PTX/CEP nanoparticle

spectively) represent the coded values of the polymer concentration, surfactant concentration and stirring time, respectively. The fitting results indicated that the optimized nanoparticles with high EE, high DL percentage and small mean diameter were obtained at the polymer concentration of 48 mg, surfactant concentration of 0.45% and stirring time of 60 min, respectively. Table 3 depicts the experimental values of the two batches prepared within the optimum range that are very close to the predicted values with low percentage bias, suggesting that the optimized formulation was reliable and reasonable.

Particle size, polydispersity index and zeta potential measurement

The mean PS of the nanoparticles was 198 nm with a polydispersity index of 0.194 ± 0.025. A narrow polydispersity index (PI) means that the colloidal suspensions are homogeneous in nature. The zeta potential of the nanoparticles was found to be -25mV, and it was sufficiently high to form stable colloidal nanosuspension.

Anticancer efficacy of PTX/CEP nanoparticles against MKN45 cells

In the *in vitro* cytotoxicity test, blank nanoparticles were demonstrated to be nearly nontoxic to MKN45 cells with 15 % inhibition rate at a high concentration of 800μg/mL. The concentration of CEP was fixed to 2 μM, a nontoxic dose which led to <5% cell death. Free PTX and PTX/CEP nanoparticles had a dose-response effect against MKN45 cells. Moreover, PTX/CEP nanoparticles induced significantly more cell death than free PTX at a series of equivalent doses. The half maximal inhibitory concentration value of PTX in cells receiving PTX/CEP nanoparticles (11.07 ± 0.97 nM) was significantly lower compared to cells receiving free PTX (18.50 ± 1.35 nM).

In vivo tumor inhibition study

The changes of xenograt tumor volume are shown in Figure 2. After 12 days of drug administration, the mice were sacrificed and the xenografted tumors were excised completely. The tumor size and weight were measured to calculate the tumor inhibition rate (TIR) as follows:

TIR = average tumor weight (volume) of control group - average tumor weight (volume) of test group]/average tumor weight (volume) of control group × 100%.

The PTX or PTX/CEP nanoparticle groups significantly reduced the tumor volume as compared with the control group (p<0.05). Moreover, the PTX/CEP nanoparticles were superior to the pure PTX group (p<0.05) in terms of tumor

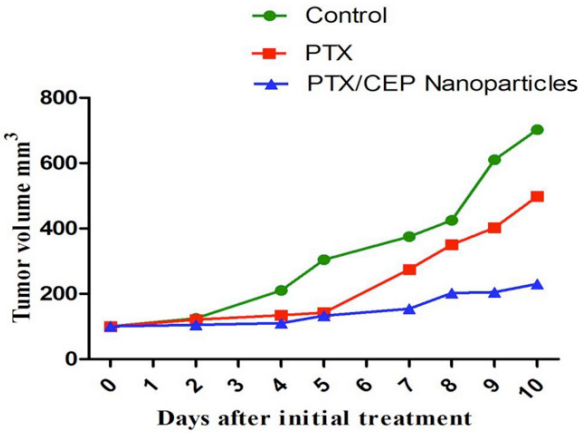

Figure 2. Kaplan-Meier survival curves in relation to tumor volume as a function of time (p<0.05).

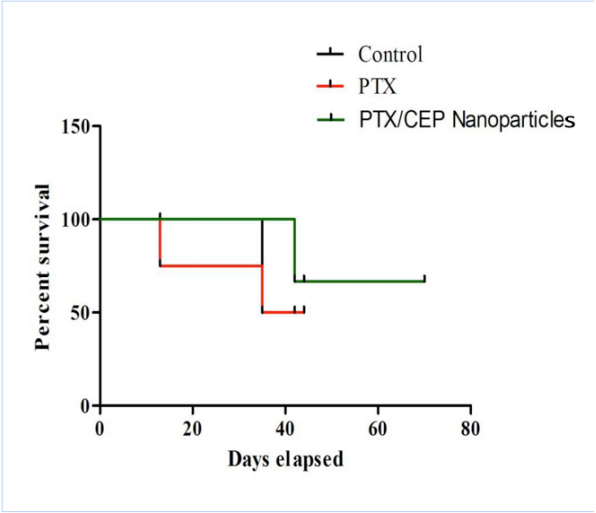

Figure 3. Kaplan-Meier survival curves of gastric cancer xenograft bearing mice (p<0.01).

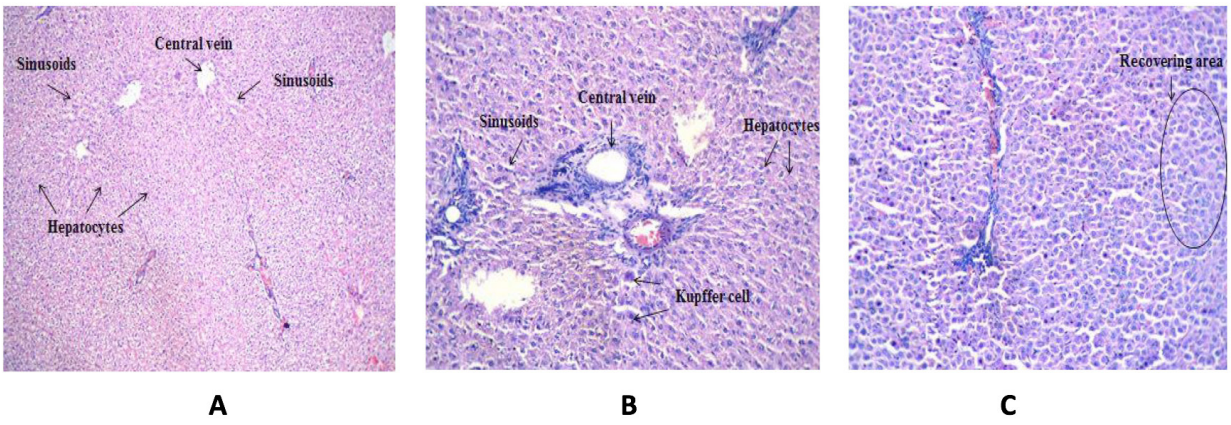

Figure 4. Tumor slices stained with hematoxylin and eosin. The slices were prepared from the margin of xenografts, and the necrotic area in the PTX/CEP nanoparticle group is significantly increased compared with that of the other groups. **A:** (normal control) sheets of prominent hepatocytes, sinusoids & central vein; **B:** (tumor control) hepatic congestion at sinusoids and the portal vessel, pe¬ricentre globular micro-steatosis, Kupffer cell proliferation and hepatocyte diffuse necrosis; **C:** (PTX/CEP nanoparticle treated) No hepatic congestion at sinusoids and the portal vessel, pe¬ricentre globular micro-steatosis, no Kupffer cell proliferation and no hepatocyte diffuse necrosis (magnification x100).

growth inhibition. Furthermore, the size-based TIR values of the PTX and PTX/CEP nanoparticle groups on day 12 after initial drug administration were about 39.8 and 73.2%, respectively (Table 4). Their weight-based TIR values were about 22.2 and 62.8%, respectively. PTX/CEP nanoparticles showed the best tumor growth inhibitory effect compared with the free PTX in a time-dependent manner.

Mice survival analysis

A total of 75 mice were randomly divided into three groups and used for survival analysis. The subcutaneous tumors were measured every two days. As shown in Figure 2, the drug groups exhibited significant tumor growth inhibition efficacy. After 75 days of initial treatment, when the survival analysis was censored, all mice in the control and PTX groups had died, while 3 mice survived in the PTX/CEP group. The median/mean survival time of the groups was compared using log-rank test (Table 5) and the difference in survival time between the PTX/CEP nanoparticles and the other groups was statistically significant (p<0.05). In particular, the tumor-bearing mice in the drug groups showed a prolonged survival time compared with the control group (Figure 3)

and the PTX/CEP nanoparticles were significantly more effective than PTX alone.

The growth of cancer xenografts in mice was delayed after the administration of PTX. Interestingly, some mice experienced nearly complete regression of their xenografts after treatment with PTX/CEP nanoparticle at an equivalent PTX dose of 20 mg/kg, which implies that the composite PTX/CEP nanoparticles were superior to PTX alone and warrant further preclinical research as a promising agent in chemotherapy for gastric cancer. It should be noted that the PTX formulations used in this study have shown different orders of antitumor activity in vitro and in vivo. In theory, the faster clearance of free PTX from the body reduced the amount of drug entering cancer cells, while for nanoscale PTX/CEP nanoparticles enhanced antitumor efficacy was noticed, which may be caused by the "shielding" effect of the PEG corona, combined with enhanced endocytosis.

Histopathological examination

The hematoxylin and eosin staining was performed to assess the margin of the excised tumor xenografts where the blood supply is theoretically better than that within the tumor. As shown in Figure 4, the areas of tissue necrosis (indicated by straight arrows) significantly increased in the PTX/CEP nanoparticle group compared with the others, which further demonstrated the enhanced antitumor efficacy of PTX/CEP. In addition, a few neutrophils, lymphocytes, and macrophages were found around or within the necrotic area of the tumor tissue sections, which evidences phagocytosis and a clearance reaction after cell apoptosis [19].

Discussion

PTX could be a successful chemotherapeutic agent only if its side effects against normal tissues and the events caused by intolerable solvents could be reduced. Different methods have been designed to maximize localization of the drug to the tumor while minimizing systemic toxicity. Recently, drug delivery systems have been engineered for the delivery of PTX [20-23]. However, in a preliminary study, it was found that PTX-loaded nanoparticles with amphiphilic copolymer as the carrier were unstable in the aqueous phase and easy to aggregate. It was previously reported that CEP could effectively stabilize PTX-loaded nanoparticles when it was co-encapsulated with PTX [10,11]. In the current study, the loading efficiency of PTX/CEP nanoparticles was optimized by central composite rotatable design-response surface methodology. As shown in Figure 1, the polymer concentration and surfactant concentration greatly influenced the loading efficiency of the co-drug loaded nanoparticles. It was observed that the highest DL and EE were achieved with optimized assay conditions of polymer concentration of 48 mg, surfactant concentration of 0.45% and stirring time of 60 min.

In addition, it was demonstrated that CEP could synergistically enhance the anticancer effect of PTX against gastric cancer cells [10-12]. Hence, co-encapsulation of PTX/CEP into nanoparticles not only shows better stability than PTX-loaded nanoparticles but also retains the synergistic anti-cancer efficiency of PTX and CEP. The *in vitro* cytotoxicity test indicated that a nearly nontoxic dose of CEP significantly improved the cytotoxicity of PTX whether or not delivered by nanoparticles. The findings reported in the current studies demonstrated the anticancer potential of PTX/CEP nanoparticles in gastrointestinal cancer.

In vivo evaluation in the mouse model showed superior antitumor efficacy of PTX/CEP nanoparticles when delivered by intravenous injection. The characteristic pharmacodynamics and pharmacokinetics of intra-tumoral delivery determines the therapeutic efficacy of PTX/CEP nanoparticles. As a site-specific delivery to a tumor nodule, the co-drug loaded nanoparticles will accordingly induce a higher local drug concentration than systemic delivery. Although PTX/CEP administered intravenously cannot achieve as high an initial concentration as free drugs, the sustained release of the encapsulated drugs is capable of delivering its anti-tumor efficacy constantly. Therefore, it is highly reasonable that released drugs from the intra-tumorally delivered nanoparticles remain in the interstitial space of the tumor for a longer time compared to normal tissue and exert a protracted tumor eliminating effect locally.

The planned modifications of the co-drug loaded nanoparticles utilized in this study are under active consideration as a part of ongoing research in authors' laboratory. Further, development on the basis of multidrug administration by nanoparticles will be fully reviewed in human orthotopic xenograft models in order to further expand the parameters of this current research. Thus, together with the current findings, it is of great value in future experiments to focus on co-drug delivery systems.

Conclusion

This study reported a stable co-drug loaded nanoparticles, formed by amphiphilic methoxy PEG-PCL block copolymers. PTX and CEP were co-incorporated into the nanoparticles with relatively high loading efficiency. In vitro studies proved the superior cytotoxicity of PTX/CEP nanoparticles in a dose-dependent manner against MKN45 cells. *In vivo* evaluation showed that PTX/CEP nanoparticles, when delivered intravenously, exhibited significantly improved antitumor efficacy and subsequently increased the overall survival in an established MKN45-transplanted mouse model.

Acknowledgement

The authors express their gratitude to the Department of Gastrointestinal Surgery, Shandong Provincial Qian Foshan Hospital, Jinan, Shandong, China and the Department of Surgery, PLA Hospital, Jinan Military Region, Jinan, Shandong, China.

References

1. Jemal A, Bray F, Center MM, Ferlay J, Ward E, Forman. Global cancer statistics. CA Cancer J Clin 2011;61:69-90.
2. Isobe Y, Nashimoto A, Akazawa K. Gastric cancer treatment in Japan: 2008 annual report of the JGCA nationwide registry. Gastric Cancer 2011;14:301-316.
3. Yamada J, Kitayama J, Tsuno NH. Intra-peritoneal administration of paclitaxel with non-animal stabilized hyaluronic acid as a vehicle: a new strategy against peritoneal dissemination of gastric cancer. Cancer Lett 2008;272:307-315.
4. Bajaj G, Yeo Y. Drug delivery systems for intraperitoneal therapy. Pharm Res 2010;27:735-738.
5. Diaz JF, Andreu JM. Assembly of purified GDP-tubulin into microtubules induced by taxol and taxotere: reversibility, ligand stoichiometry, and competition. Biochemistry 1993;32:2747-2755.
6. Strumberg D, Erhard J, Harstrick A. Phase I study of a weekly 1 h infusion of paclitaxel in patients with unresectable hepatocellular carcinoma. Eur J Cancer 1998;34:1290-1292.
7. Chao Y, Chan WK, Birkhofer MJ. Phase II and pharmacokinetic study of paclitaxel therapy for unresectable hepatocellular carcinoma patients. Br J Cancer 1998;78:34-39.
8. Dorr RT. Pharmacology and toxicology of Cremophor EL diluent. Ann Pharmacother 1994;28:11-14.
9. Bissery MC, Nohynek G, Sanderink GJ, Lavelle F. Docetaxel (Taxotere): a review of preclinical and clinical experience. Part I: preclinical experience. Anticancer Drugs 1995;6:339-355.
10. Ikeda R, Che XF, Yamaguchi T. Cepharanthine potently enhances the sensitivity of anticancer agents in K562 cells. Cancer Sci 2005;96:372-376.
11. Harada K, Ferdous T, Itashiki Y. Effects of cepharanthine alone and in combination with fluoropyrimidine anticancer agent, S-1, on tumor growth of human oral squamous cell carcinoma xenografts in nude mice. Anticancer Res 2009;29:1263-1270.
12. Rogosnitzky M, Danks R. Therapeutic potential of the biscoclaurine alkaloid, cepharanthine, for a range of clinical conditions. Pharmacol Rep 2011;63:337-347.
13. Li X, Li R, Qian X et al. Superior antitumor efficiency of cisplatin-loaded nanoparticles by intratumoral delivery with decreased tumor metabolism rate. Eur J Pharm Biopharm 2008;703:726-734.
14. Shao J, Zheng D, Jiang Z et al. Curcumin delivery by methoxy polyethylene glycol-poly (caprolactone) nanoparticles inhibits the growth of C6 glioma cells. Acta Biochim Biophys Sin (Shanghai) 2011;43:267-274.
15. Herold DA, Keil K, Bruns DE. Oxidation of polyethylene glycol by alcohol dehydrogenase. Biochem Pharmacol 1989;38:73-76.
16. Maeda H: The enhanced permeability and retention (EPR) effect in tumor vasculature: the key role of tumor-selective macromolecular drug targeting. Adv Enzyme Regul 2001;41:189-207.
17. Idani H, Matsuoka J, Yasuda T, Kobayashi K, Tanaka N. Intra-tumoral injection of doxorubicin (Adriamycin) encapsulated in liposome inhibits tumor growth, prolongs survival time and is not associated with local or systemic side effects. Int J Cancer 2000;88:645-651.
18. Li X, Lu X, Xu H. Paclitaxel/tetrandrine coloaded nanoparticles effectively promote the apoptosis of gastric cancer cells based on oxidation therapy. Mol Pharm 2012;9:222-229.
19. Ahn JH, Kim YP, Lee YM, Seo EM, Lee KW, Kim HS. Optimization of microencapsulation of seed oil by response surface methodology, Food Chemistry 2008;107:98-105.
20. Jersmann HP, Ross KA, Vivers S. Phagocytosis of apoptotic cells by human macrophages: analysis by multiparameter flow cytometry. Cytometry A 2003;51:7-15.
21. Ma X, Wang H, Jin S, Wu Y, Liang XJ. Construction

of paclitaxel-loaded poly (2-hydroxyethyl methacrylate)-g-poly (lactide)-1, 2-dipalmitoyl-sn-glycero-3-phosphoethanolamine copolymer nanoparticle delivery system and evaluation of its anticancer activity. Int J Nanomedicine 2012;7:1313-1328.

22. Wang J, Mongayt D, Torchilin VP. Polymeric micelles for delivery of poorly soluble drugs: preparation and anticancer activity in vitro of paclitaxel incorporated into mixed micelles based on poly (ethylene glycol)-lipid conjugate and positively charged lipids. J Drug Target 2005;13:73-80.
23. Shenoy D, Little S, Langer R, Amiji M. Poly (ethylene oxide) - modified poly (β-amino ester) nanoparticles as a pH-sensitive system for tumor-targeted delivery of hydrophobic drugs. 1. In vitro evaluations. Mol Pharm 2005;2:357-366.